

# A Highly Reproducible SU-8 Cantilever Platform with Integrated Strain Sensor Fabricated via Deep RIE for Quantitative Mechanical Sensing

Hong-Mo Koo<sup>1,2,\*</sup>, Dong-Su Kim<sup>1,\*</sup>, Dae-Yun Lim<sup>1,2</sup>, Young Baek Kim<sup>1,+</sup>, and Dong-Weon Lee<sup>2,3,4,+</sup>

<sup>1</sup>National Center for Nano Process & Equipments, Korea Institute of Industrial Technology (KITECH), Republic of Korea

<sup>2</sup>MEMS and Nanotechnology Laboratory, School of Mechanical Engineering, Chonnam National University, Republic of Korea

<sup>3</sup>Advanced Medical Device Research Center for Cardiovascular Disease, Chonnam National University, Republic of Korea

<sup>4</sup>Center for Next-generation Sensor Research and Development, Chonnam National University, Republic of Korea

 **Cite This:** *J. Sens. Sci. Technol.* Vol. 34, No. 4 (2025) 272-277

 <https://doi.org/10.46670/JSST.2025.34.4.272>

**ABSTRACT:** Drug-induced cardiotoxicity is a major cause of failure in drug development during clinical trials, which therefore necessitates reliable in vitro evaluation methods. Polymer cantilevers have emerged as promising tools for measuring cardiomyocyte contractility. However, their low fabrication reproducibility has limited their application in high-throughput screening. In this study, we present an SU-8 cantilever platform integrated with a metal strain sensor for precise monitoring of cardiomyocyte contraction. The platform is fabricated using conventional microfabrication techniques, utilizing an SU-8 photoresist as the structural material due to its low Young's modulus (~2 GPa) and high biocompatibility. To improve fabrication precision and yield, a deep reactive ion etching (DRIE) process was employed to uniformly release twelve cantilevers from a single chip. This approach significantly improved throughput and reduced process time. Each cantilever integrates a strain sensor configured in a Wheatstone bridge circuit, enabling real-time detection of mechanical deformations caused by cardiac contraction. Performance evaluation confirmed the sensor's stability, with a measured gauge factor of 2.09 and consistent displacement resolution down to 10  $\mu\text{m}$  across all devices. These results demonstrate excellent reproducibility and uniform sensing characteristics. The proposed platform offers a reliable solution for accurate, high-throughput in vitro screening of drug-induced cardiotoxicity.

**KEYWORDS:** *SU-8 cantilever, Strain sensor, MEMS, Deep RIE, Reproducibility*

## 1. INTRODUCTION

According to the World Health Organization (WHO), ischemic heart disease is the leading cause of death worldwide, accounting for approximately 13% of all deaths [1]. Numerous drugs have been developed to address this issue [2]. However, the development of new drugs requires considerable time and financial resources [3], which makes drug evaluation a critical step in the drug development pipeline.

Various devices and techniques have been proposed to evaluate drug effects [4]. Pesl et al. introduced an evaluation

method using atomic force microscopy (AFM), which, combined with a microcantilever probe, enables high-precision measurement of cardiomyocyte contractility and beating rate [5]. However, AFM is limited by its low throughput because it can only evaluate a single cell at a time. Beussman et al. proposed an optical method using a Polydimethylsiloxane (PDMS) micropost array [6], but this approach is labor-intensive and requires manual analysis. Qian et al. developed an impedance-based method for monitoring cardiomyocyte contraction [7], which allows real-time and long-term analysis, but involves direct current flow through cells, potentially causing side effects.

To overcome these limitations, several cantilever-based platforms integrated with strain sensors have been developed. Lind et al. employed multi-material 3D printing to fabricate such platforms [8], although the resulting cantilevers were relatively thick, which reduced sensitivity. Kim et al. developed silicone rubber cantilevers with integrated crack sensors [9], offering high sensitivity and long-term stability, but exhibiting

\*These authors contributed equally to this work.

+Corresponding authors: kimmoon@kitech.re.kr, mems@jnu.ac.kr

Received : Jun. 5, 2025, Accepted : Jun. 9, 2025

This is an Open Access article distributed under the terms of the Creative Commons Attribution Non-Commercial License (<https://creativecommons.org/licenses/by-nc/3.0/>) which permits unrestricted non-commercial use, distribution, and reproduction in any medium, provided the original work is properly cited.

nonlinear output. Dong et al. used silicon-based cantilevers [10]; however, the high Young’s modulus of silicon (~150 GPa) rendered it unsuitable for detecting small cell-generated forces. PDMS-based biosensors [11] provide high biocompatibility but are not compatible with photolithography, often requiring manual bonding, which limits reproducibility.

Sun et al. proposed an SU-8-based cantilever platform [12] that exploited the biocompatibility of SU-8 and its compatibility with standard photolithography processes. However, their platform included only a few cantilevers per chip and wafer separation was performed manually, resulting in low scalability and reduced yield. Additionally, the use of a silicon oxide sacrificial layer leads to prolonged etching times, and employing SU-8 as the cantilever body material introduces structural deformation issues during long-term cell culture.

To overcome these limitations, we employed a deep reactive ion etching (DRIE) process to fabricate a multicantilever SU-8 platform that enabled simultaneous and uniform release from the wafer. Twelve cantilevers were integrated on a single chip, resulting in a yield exceeding 85%, and eliminating the need for manual separation. This fabrication strategy improves throughput, batch-to-batch repeatability, and dimensional precision. Compared with previous SU-8 cantilever platforms, our DRIE-based process enabled scalable and uniform production. The integrated strain sensors exhibited a gauge factor of 2.09 with consistent displacement resolution down to 10 μm across all devices, indicating excellent reproducibility and uniform sensing characteristics. These advancements have established the proposed platform as a promising tool for the high-throughput screening of drug-induced cardiotoxicity.

## 2. EXPERIMENTAL METHODS

### 2.1 Working Principle of the Proposed Platform

Fig. 1. illustrates the structure and operating principle of the proposed SU-8 cantilever platform integrated with a strain sensor. When an external force is applied to the free end of the cantilever (Fig. 1 (b)), mechanical displacement occurs, inducing a strain along the cantilever. The maximum strain at the fixed end,  $\epsilon_{max}$ , can be calculated using the following equation.

$$\epsilon_{max} = \frac{6 \cdot t \cdot \delta}{l^2} \tag{1}$$

In this equation,  $l$ ,  $t$ , and  $\delta$  represent the length, thickness, and displacement at the free end of the cantilever, respectively. To quantitatively measure this strain-induced deformation, a Wheatstone bridge circuit is used. The circuit consists of a metal strain sensor and fixed resistors, as shown in Fig. 1 (c). The resistance of the metal sensor,  $R$ , is governed by the following relation.

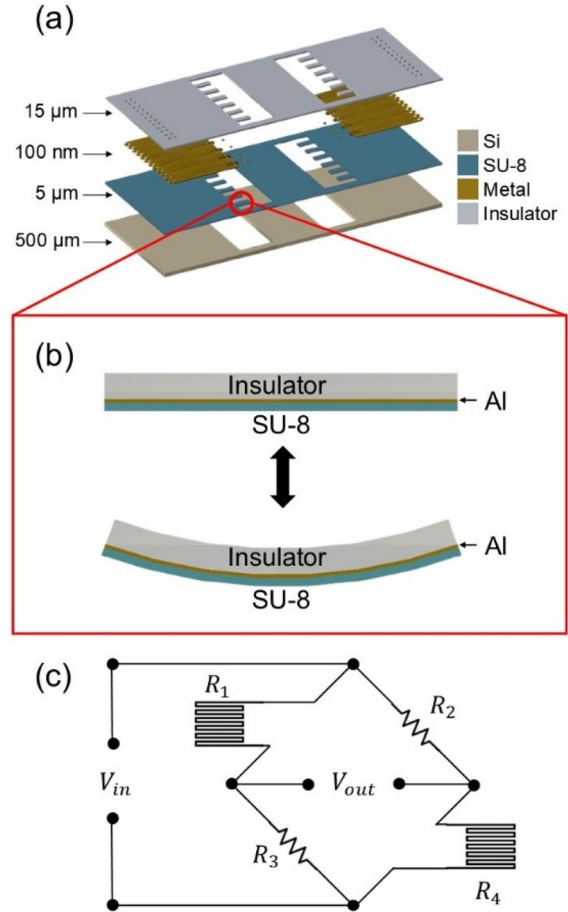


**Fig. 1.** Schematic and Operating Principles of Platform. (a) Schematic of the SU-8 cantilever platform integrated with a strain sensor. (b) Conceptual illustration of cantilever deformation under external force. (c) Schematic representation of the sensing principle for detecting cantilever deformation.

$$R = \rho \frac{L}{A} \tag{2}$$

Here,  $\rho$ ,  $L$ , and  $A$  denote the resistivity, length, and cross-sectional area of the metal, respectively. As the cantilever bends, the strain sensor located near the fixed end undergoes the same mechanical strain. This results in a change in the sensor’s length and therefore a change in resistance.

The Wheatstone bridge converts this change in resistance into a measurable output voltage. The output voltage,  $V_{out}$ , is given by the equation below.

$$V_{out} = V_{in} \left( \frac{R_3}{R_1 + R_3} - \frac{R_4}{R_2 + R_4} \right) \tag{3}$$

In this circuit,  $R_1$  and  $R_4$  are the strain-sensitive resistors. When strain is applied, variations in their resistance result in a change in  $V_{out}$ , which can be continuously monitored to detect the deformation of the cantilever (Fig. 1 (d)).

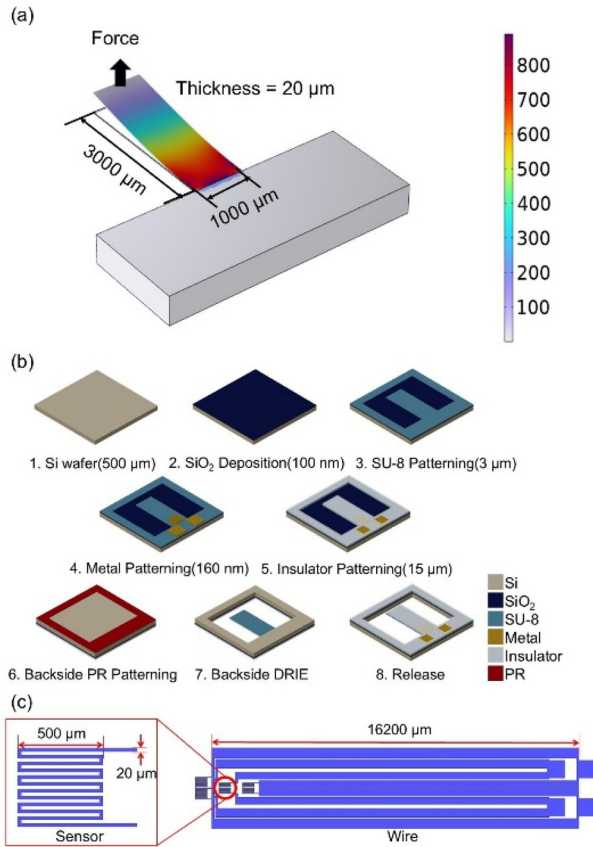


**Fig. 2.** Platform Design and Fabrication Process. (a) COMSOL simulation results showing stress distribution in the cantilever structure. (b) Schematic diagram of the fabrication process for the SU-8 cantilever platform. (c) Layout of the strain sensor and electrical interconnections.

### 2.2 Design and Fabrication

Fig. 2. illustrates the design and fabrication of the proposed SU-8 cantilever platform using an integrated strain sensor. Each cantilever was designed with dimensions of 3000 μm (length), 1000 μm (width), and 20 μm (thickness). A COMSOL simulation was conducted using these parameters to optimize sensor placement (Fig. 2 (a)). Based on the simulation results, the strain sensor was positioned within 500 μm of the fixed end, where approximately 80% of the maximum stress was concentrated. Aluminum (Al) was selected as the strain sensor material. The sensor pattern was designed with a line width of 20 μm and a thickness of 100 nm, resulting in a nominal resistance of 133 Ω. To minimize the influence of interconnect resistance on signal accuracy, the connecting wires were designed to have a resistance of approximately 24 Ω, corresponding to 20% of the sensor resistance.

The fabrication process is shown in Fig. 2 (b). A 100 nm thick SiO<sub>2</sub> layer was first deposited on the surface of a double-sided polished (DSP) silicon wafer by inline sputtering. A

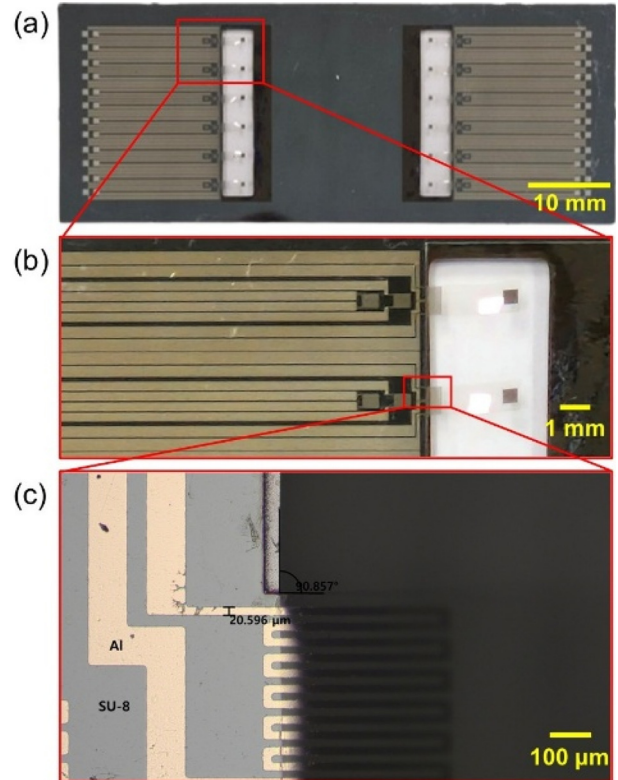


**Fig. 3.** Fabricated Platform Image. (a) Optical image of the fabricated SU-8 cantilever array. (b) Magnified view of the strain sensor region, highlighting the patterned metal interconnects. (c) High-magnification image of the patterned aluminum (Al) strain sensor on the SU-8 cantilever.

3 μm thick SU-8 6002 layer was then patterned by photolithography to form the initial cantilever structure. A Molybdenum–Aluminum–Molybdenum (Mo–Al–Mo) tri-layer (50 nm / 100 nm / 10 nm) was subsequently deposited on the SU-8 structure using the same sputtering system. The strain sensor pattern was defined using an AZ-GXR 601 photoresist as a mask and etched via inductively coupled plasma (ICP) etching. A 17 μm thick insulating layer was formed using SU-8 3010 by photolithography, yielding a total cantilever thickness of 20 μm. To release the cantilever platform, JSR THB-126N photoresist was applied as a backside mask. The wafer was then etched to a depth of 500 μm using deep reactive ion etching (DRIE), completing the fabrication process (Fig. 2 (c)).

Fig. 3. shows the structural characteristics of the fabricated SU-8 cantilever platform. The optical image of the entire device shows an array of SU-8 cantilevers integrated with strain sensors (Fig. 3 (a)). The strain sensor region, including the metal interconnects patterned in a Wheatstone bridge configuration, is clearly visible in the magnified view (Fig. 3 (b)). A high-magnification image reveals the aluminum (Al) strain gauge fabricated on the SU-8 cantilever (Fig. 3 (c)). The sensor lines were designed with a nominal width of 20 μm, while the

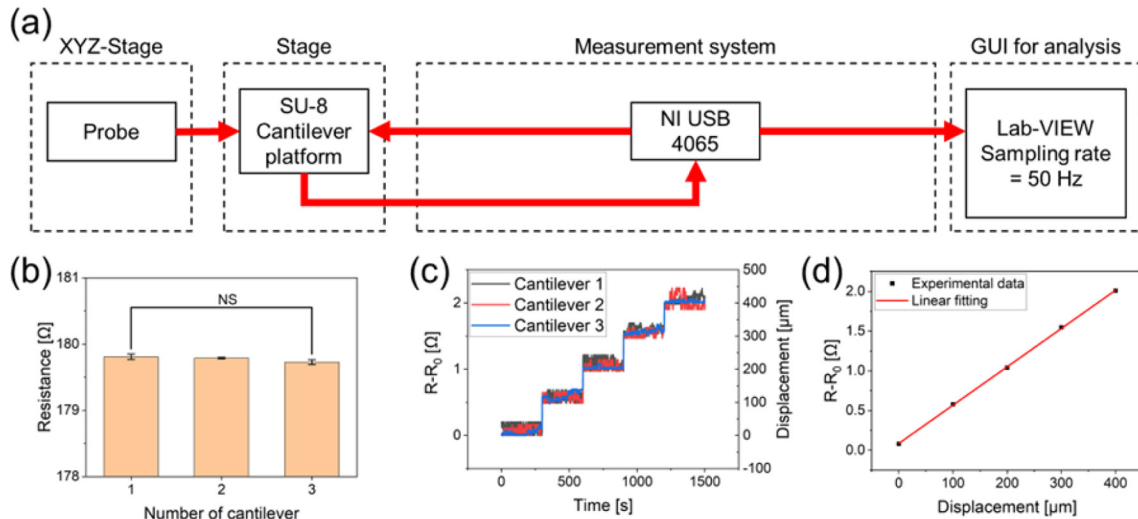


**Fig. 4.** Methods and Results of Resistance Experiments. (a) Schematic of the experimental setup and measurement method for evaluating resistance changes under displacement. (b) Bar chart showing the initial resistance values measured from three different cantilevers. (c) Real-time resistance variation with displacement for each cantilever. (d) Averaged resistance variation as a function of applied displacement.

actual fabricated width was measured to be approximately 20.6  $\mu\text{m}$ , resulting in a dimensional error of 3.0%. This small deviation confirms the high precision and reproducibility of the microfabrication process.

### 3. RESULTS AND DISCUSSIONS

#### 3.1 Measurement of Resistance Change with Displacement

An experiment was conducted to induce controlled displacement at the free end of the cantilever and measure the resulting changes in resistance. Fig. 4 (a) shows a schematic of the experimental setup used for the real-time monitoring of resistance under mechanical deformation.

The cantilever platform was mounted onto a measurement stage and displacements were applied using a probe capable of moving along the x, y, and z axes. The resistance changes in the strain sensors were measured in real time using a LabVIEW-based data acquisition system (USB 4065, National Instruments Inc., Austin, TX, USA). The measurement system was configured to sample at 50 Hz to capture the dynamic resistance changes in the sensors (Fig. 4 (a)). Fig. 4 (b) shows the initial resistance values of the three different cantilevers. The average resistance was 179.8  $\Omega$ , which closely matches the designed resistance of 181  $\Omega$ , with a percentage error of 0.662%. The analysis of variance (ANOVA) confirmed that there were no statistically significant differences among the three sensors ( $p > 0.05$ ). Fig. 4 (c) shows the real-time resistance response of each cantilever during displacement. The sensors exhibited consistent trends in the resistance variation

with displacement. Fig. 4 (d) displays the averaged resistance variation corresponding to the applied displacement. The gauge factor (GF) was calculated using the following equation:

$$GF = \frac{\Delta R/R}{\varepsilon} \quad (4)$$

Here,  $GF$  denotes the gauge factor, and  $\Delta R$ ,  $R$ , and  $\varepsilon$  represent the change in resistance, initial resistance, and strain, respectively. Using Eqs. (1) and (4), the gauge factor was determined to be 2.0924. This value is in close agreement with the known gauge factor of aluminum, which is approximately 2.

#### 3.2 Changes in the SU-8 Cantilever Platform under Thermal Conditions

The proposed SU-8 cantilever platform integrated with a strain sensor is intended for use in cell culture environments maintained at 37°C. To verify the thermal stability, measurements were conducted under temperature conditions similar to those expected for biological applications.

As shown in Fig. 5 (a), the sensor platform was placed on a hot plate and fixed at a fixed position. A voltage was applied, and the output signal was monitored using the same acquisition setup. Measurements were performed on three cantilevers at room temperature, followed by additional measurements at 40°C after thermal stabilization. Fig. 5 (b) shows the baseline signal trends over time at both temperatures. The results indicated that the platform maintained a consistent and stable signal under both conditions, with no noticeable thermal drift. Fig. 5 (c) shows the average baseline values obtained from

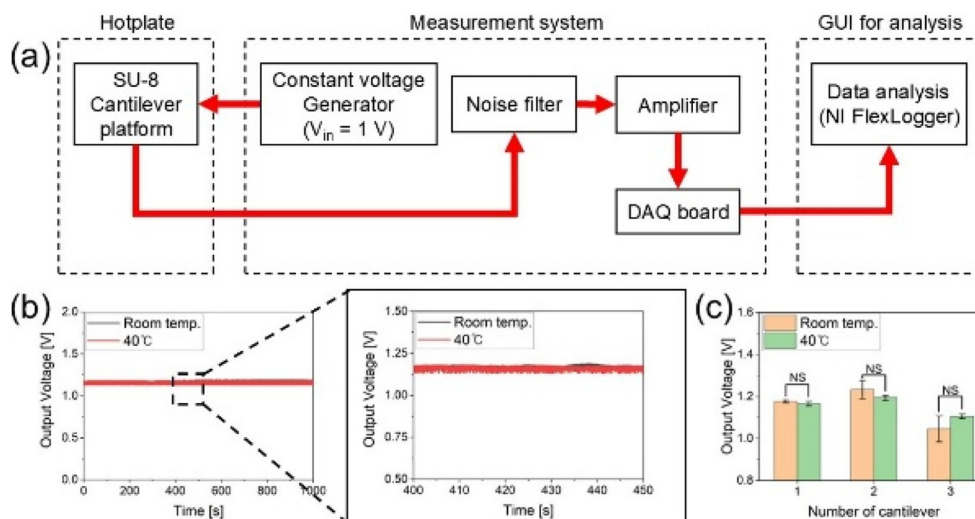


**Fig. 5.** Methods and Results of Temperature Experiments. (a) Schematic of the measurement setup and data acquisition process under thermal conditions. (b) Baseline signals recorded at room temperature and 40°C. (c) Bar chart comparing the average baseline values at room temperature and 40°C.

three devices at each temperature. Analysis of variance (ANOVA) confirmed that the differences between the two groups were not statistically significant ( $p > 0.05$ ), demonstrating the thermal stability of the platform under conditions mimicking the cell culture environment.

### 3.3 Measurement of Voltage Change with Displacement

The cantilever platform was mounted on a measurement stage and controlled displacement was applied using a probe mounted on a motorized XYZ translation stage. An input voltage of 1 V was applied during the measurements, and the output voltage was recorded as the displacement was applied to the free end of the cantilever. Fig. 6 (a) shows the real-time voltage responses of the three cantilevers under the displacement conditions. The voltage changes were clearly distinguishable, with a minimum displacement resolution of 10  $\mu\text{m}$ , and consistent trends were observed across all samples. Fig. 6 (b) shows the average voltage variation as a function of displacement, which exhibits a linear relationship,

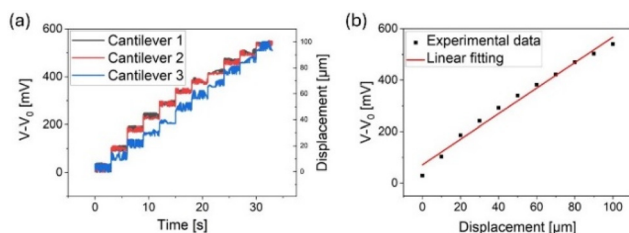


**Fig. 6.** Results of Voltage Experiments. (a) Real-time voltage variation in response to displacement for three cantilevers. (b) Averaged voltage output as a function of applied displacement, showing linearity.

confirming the suitability of the platform for quantitative mechanical sensing.

## 4. CONCLUSION

In this study, the productivity and reproducibility were enhanced through deep reactive ion etching (DRIE), resulting in yields exceeding 85%. The performance of the proposed SU-8 cantilever platform integrated with the strain sensor was experimentally validated. The platform exhibited stable baseline signals, even after prolonged exposure to the thermal environment. The initial resistance measurements showed minimal deviation from the designed values, and the strain-sensing experiments produced a gauge factor close to that of aluminum, indicating the high reliability and accuracy of the fabricated sensor system. Voltage-response measurements further confirmed the high sensitivity and linearity of the platform with respect to displacement, demonstrating its suitability for quantitative mechanical sensing. These characteristics are particularly advantageous for future applications such as the evaluation of the contractile force of cardiomyocytes. Although this platform has not been directly applied to measure cardiomyocyte contractility, further studies under actual cell culture conditions are required to verify its applicability. If successful, the SU-8 cantilever platform could serve as a promising tool for high-throughput drug screening and cardiotoxicity assessments.

### CRediT Authorship Contribution Statement

**Hong-Mo Koo:** Conceptualization, Data curation, formal analysis, Investigation, Visualization, Writing of the original

draft. **Dong-Su Kim:** Conceptualization, Funding acquisition, Investigation, Methodology, Validation, Writing, review, and editing. **Dae-Yun Lim:** Investigation, Methodology. **Young Baek Kim:** Funding acquisition, Resources, Supervision, Validation. **Dong-Weon Lee:** Methodology, Funding acquisition, Resources, Supervision, Validation.

### Declaration of Competing Interest

The authors declare that they have no competing financial interests or personal relationships that may have influenced the work reported in this study.

### Acknowledgements

This work was supported by the National Research Foundation of Korea (NRF) grant funded by the Korean Government (MSIT) (RS-2022-00165505, RS-2022-NR072456). This work was supported by the Korea Planning & Evaluation Institute of Industrial Technology(KEIT) and Ministry of Trade, Industry & Energy(MOTIE) of the Republic of Korea (RS-2023-00257663).

## REFERENCES

- [1] World Health Organization(WHO), The top 10 causes of death. <https://www.who.int/news-room/fact-sheets/detail/the-top-10-causes-of-death>, 2024 (accessed 5 June 2025).
- [2] V.J. Wirtz, W.A. Kaplan, G.F. Kwan, R.O. Laing, Access to medications for cardiovascular diseases in low-and middle-income countries, *Circulation* 133 (2016) 2076–2085.
- [3] A.P. Prashant, Global challenges in cardiovascular drug discovery and clinical trials, *Mol. Biol.* 6 (2017) 1000193.
- [4] K.W. Cho, W.H. Lee, B.-S. Kim, D.-H. Kim, Sensors in heart-on-a-chip: A review on recent progress, *Talanta* 219 (2020) 121269.
- [5] M. Pesl, J. Pribyl, I. Acimovic, A. Vilotic, S. Jelinkova, A. Salykin, et al., Atomic force microscopy combined with human pluripotent stem cell derived cardiomyocytes for biomechanical sensing, *Biosens. Bioelectron.* 85 (2016) 751–757.
- [6] K.M. Beussman, M.L. Rodriguez, A. Leonard, N. Taparia, C.R. Thompson, N.J. Sniadecki, Micropost arrays for measuring stem cell-derived cardiomyocyte contractility, *Methods* 94 (2016) 43–50.
- [7] F. Qian, C. Huang, Y.-D. Lin, A.N. Ivanovskaya, T.J. O'Hara, R.H. Booth, et al., Simultaneous electrical recording of cardiac electrophysiology and contraction on chip, *Lab Chip* 17 (2017) 1732–1739.
- [8] J.U. Lind, T.A. Busbee, A.D. Valentine, F.S. Pasqualini, H. Yuan, M. Yadid, et al., Instrumented cardiac microphysiological devices via multimaterial three-dimensional printing, *Nat. Mater.* 16 (2017) 303–308.
- [9] D.S. Kim, Y.W. Choi, A. Shanmugasundaram, Y.J. Jeong, J. Park, N.E. Oyunbaatar, et al., Highly durable crack sensor integrated with silicone rubber cantilever for measuring cardiac contractility, *Nat. Commun.* 11 (2020) 535.
- [10] M. Dong, N.E. Oyunbaatar, P.P. Kanade, D.S. Kim, D.W. Lee, Real-time monitoring of changes in cardiac contractility using silicon cantilever arrays integrated with strain sensors, *ACS Sens.* 6 (2021) 3556–3563.
- [11] D.S. Kim, Y.J. Jeong, B.K. Lee, A. Shanmugasundaram, D.W. Lee, Piezoresistive sensor-integrated PDMS cantilever: A new class of device for measuring the drug-induced changes in the mechanical activity of cardiomyocytes, *Sens. Actuators B Chem.* 240 (2017) 566–572.
- [12] H. Sun, D.-S. Kim, A. Shanmugasundaram, J.-Y. Kim, E.-S. Kim, B.-K. Lee, et al., Enhancing cardiomyocytes contraction force measuring in drug testing: Integration of a highly sensitive single-crystal silicon strain sensor into SU-8 cantilevers, *Biosens. Bioelectron.* 243 (2024) 115756.